pH sensitivity of edge-gated graphene field-effect devices with covalent edge-functionalization

Tilmann J. Neubert[1,2], Janina Krieg[1], Anur Yadav[1,2], Kannan Balasubramanian[1,2*]

[1]Department of Chemistry, Humboldt-Universität zu Berlin, Berlin, Germany.

[2]School of Analytical Sciences Adlershof (SALSA) & IRIS Adlershof, Humboldt-Universität zu Berlin, Berlin, Germany.

Corresponding author e-mail: nano.anchem@hu-berlin.de

ABSTRACT

We present here a new strategy for a field-effect device, termed graphene edge field-effect transistor (GrEdge-FET), where a micron-wide graphene monolayer is gated exclusively through its edge in an aqueous environment. This is achieved by passivating the basal plane selectively using photolithography. We observe a field-effect behavior in buffer solutions with an ON/OFF ratio of nearly 10 in a small gate-voltage range (+/- 0.5 V) without any need for complex nanofabrication or specialized electrolytes. We attribute this effect to the electrical double layer capacitance at the edge-electrolyte interface, which efficiently gates the entire graphene sheet although it acts only at the edge. We demonstrate that GrEdge-FET devices find applications as pH sensors. Through diazonium electrochemistry, the edges are functionalized persistently with substituted phenyl moieties, which renders the devices with a higher pH sensitivity than classical graphene FETs. Moreover, since only the edge is modified, the favorable field-effect behavior is preserved, despite the covalent nature of attachment of the functional groups.

Keywords: graphene nanoribbons, graphene edge, sensing, covalent modification, 2D materials

INTRODUCTION

Individual sheets of the two-dimensional (2D) material graphene have been integrated into field-effect devices with promising applications in (opto)electronics, sensing and radio frequency applications. [1-7] In most of the graphene field-effect transistors (GFETs), the field-effect occurs by gating the entire 2D surface of a single sheet. Edges present at the sheet ends or at the holes and cracks often play an ancillary role in the field-effect characteristics. Several approaches have been demonstrated to obtain GFET devices with enriched edges. [8] Graphene nanoribbon FETs have been realized, where the width of the graphene channel bears only a few nm. [9-13] Other attempts are based on the introduction of nanostructured defects in the basal plane, such as pores, antidot lattices or the fabrication of quantum dots. [14-17] Minimizing the amount of the basal plane increases the influence of the edge in the overall device characteristics. For example, in the case of nanoribbons this is achieved by decreasing the ribbon width, while in superlattices the proportion of edges is increased by etching holes in the graphene sheet. [18-19] However, in all these cases, although the edge effects dominate the field-effect response, the contribution due to the gating of the basal plane was not excluded completely. Up until now, exclusive gating of the graphene edge is yet to be explored.

The ability to address the edge of graphene selectively is of extraordinary interest, as it represents a one-dimensional (1D) line defect in the 2D material. [8, 20-22] The specialized nature of the monolayer graphene edge has been in the focus of several recent investigations. [23-29] Since it is not feasible to obtain a free-standing atomic carbon edge, a certain portion of the basal plane needs to be present in order to support the edge. For electrochemical studies in a liquid environment, the capability to address the edge of a single graphene sheet exclusively has been demonstrated in a few occasions. [23-27, 29] In these works, exclusive exposure of the graphene edge to the electrolyte was achieved by protecting a part of the basal plane (e.g. with a photoresist) and etching or cutting away the remaining open part of the basal plane. In several of these examples, the graphene edge has been investigated to evaluate its electrocatalytic

activity or the possibility of electrochemical sensing. [23-24, 27-28, 30-32] The graphene edge termination is of a random nature in these edge electrodes. Previously, we have realized isolated graphene edge (GrEdge) electrodes, using which we were able to decipher the electron transfer properties specific to the graphene edge in detail. [23] Due to its nanoscale nature and the occurrence of low background currents, comparatively low concentrations of electroactive species could be detected. Apart from electrochemistry, field-effect detection is also a suitable transduction method to sense analyte species in liquid. [5, 33]

It is intriguing to evaluate if a field-effect is obtainable by exclusively gating the 1D edge of a graphene sheet. In this context, side-gated GFETs have been experimented in the dry state before, where the field-effect characteristics were measured by placing the gate electrode on the side of a graphene sheet. [34-37] The spacing between the side gate and the graphene channel was in the range of 95 – 500 nm, which requires the use of electron beam lithography. The electric field from the side gate influences the field-distribution only within a certain width (a few tens of nm) of the graphene channel, while the bulk of the channel remained unaffected by the gate. [34, 37] In order to modulate the charge carrier concentration across the entire graphene channel, nanoribbons of sub-10 nm width had to be deployed, which needed elaborate nanofabrication. [38] It is clear from these studies that there is a limit to the electric field strength that can be achieved with the side gate (in air or in vacuum), as dictated by fabrication requirements and electrical breakdown. Here we propose a different architecture based on electrochemical gating, [5] where the FET operates in liquid and the gating happens through the electrical double layer (EDL) at the graphene edge that is exclusively in contact with the solution. The basal plane and all electrical contacts are passivated and are hence not exposed to the solution. The devices are prepared down to a feature size of around 1 micron, which do not require any specialized nanolithography. Gating through the EDL is known to be highly efficient due to the high capacitance per unit area obtainable at the graphene-electrolyte

interface. [39] We observe that our strategy allows for gating the entire graphene channel (with a width up to a few microns) only through the edge.

Electrochemically gated GFETs have been used for pH sensing in several occasions. [9, 40-45] Here, the signal is generated due to changes in the electrical characteristics of the GFET device brought about by the protonation equilibrium of ionizable groups at the graphene-liquid interface. [7, 9, 40, 43-44] Therefore, unmodified GFETs free of residues and contamination show limited pH sensitivity (< 10 mV/pH) at relevant ionic strength. [40-41, 44] The pH-sensitivity can be improved by controlled chemical modification of the graphene surface. [5, 40, 46] There is a couple of tradeoffs, which dictate the type of modification procedure that can be used in GFET pH sensors. Non-covalent modification or depositing a chemically modified heterostructure provides comparatively higher coverage of functional groups without affecting the conductivity in graphene. [40, 44] However, in some cases the stability of the attached functionalities can be rather limited. On the other hand, covalent attachment is more advantageous since the groups are attached persistently to the graphene surface. [47] The drawback with this approach is that, at least in classical GFETs, covalent modification inadvertently leads to an increase in overall resistance and a decrease in intrinsic charge carrier mobility. [48-49] In this work, we propose the possibility of a GFET with just a 1D edge, which is active for interfacial interactions, and consequently opens new possibilities. Since the protected basal plane is immune to functionalization, it is worthwhile exploring the prospects of covalent chemical modification exclusively at the edge on the pH sensitivity. With this motivation, we first present the pH sensing capability of our GrEdge-FETs and subsequently, the improvement in pH sensing performance obtained by modifying the edge covalently using diazonium electrochemistry. The covalent modification has a minimal detrimental effect on the field-effect characteristics (such as ON/OFF ratio and ON resistance). Hence, covalently functionalized GrEdge-FETs may be considered a new class of devices that are promising for robust and routine sensing applications.

RESULTS AND DISCUSSION

The general idea behind the realization of an edge-gated graphene FET or GrEdge-FET revolves around the exclusive exposure of the edge of a graphene sheet to the gating medium, which in our case is the electrolyte solution. Since it is not possible to obtain a freestanding atomic line edge under ambient conditions, a certain portion of the basal plane region needs to be present between the source and the drain contacts in order to support the edge. This basal region will however be passivated in order to ensure that only the edge is gated by the electrolyte. Figure 1a presents the layout of such a GrEdge-FET in comparison to that of a conventional graphene FET (cGFET) in figure 1b. When a GrEdge-FET device is immersed in solution, only the edge encounters the liquid, while for a cGFET the uncovered part of the graphene basal plane is also exposed to the solution. Details of fabrication are given in the *Experimental section*. In short, CVD-grown graphene is transferred to Si/SiO_2 chips with pre-patterned Pt contacts. A graphene ribbon of size 20 by 20 μm^2 is patterned between the source and drain contacts. For obtaining a cGFET, only the metal-graphene contact regions are passivated (figure 1b). To realize a GrEdge-FET, in addition to the contact regions, a certain width of the graphene channel is additionally passivated using the negative photoresist SU-8. This width is denoted as Resist Protected Basal Width (RPBW, see figure 1a). Subsequently, the GrEdge-FET device is subjected to a mild plasma treatment to etch away the uncovered basal region and obtain an exposed edge. Figure 1c and 1d present optical images of a GrEdge-FET with an RPBW of approx. 1 μm and a cGFET with a comparable width (w) of 1.2 μm, respectively. Further proof that only the edge comes in contact with the solution is obtained from optical images taken during the fabrication process and atomic force microscopy (AFM) images (see figures S1 and S2 in Supporting Information (SI)).

In principle, the GrEdge-FET comprises of a passivated graphene ribbon, whose edge on one side is exposed and is exclusively gated by the electrolyte using an Ag/AgCl reference electrode as the gate, as depicted in figure 2a. Note that the scheme shows the edge with a certain

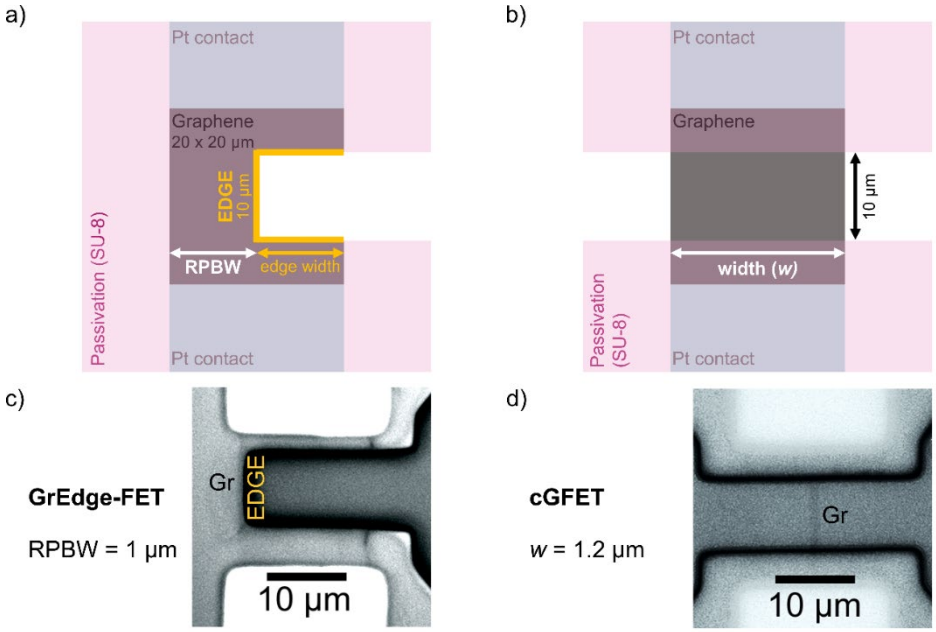

Figure 1: Device layouts. *a) Layout of the graphene edge FET (GrEdge-FET). The graphene-metal contacts and a certain width (denoted as Resist Protected Basal Width – RPBW) of the graphene channel are protected with the passivation layer (SU-8). b) Layout of a conventional GFET (cGFET) device. c),d) Optical images of c) a GrEdge-FET device with an RPBW of 1 µm and d) a cGFET device with w = 1.2 µm. That there is no exposed basal plane in the gap in the GrEdge-FET in (c) is confirmed by AFM images (see figure S2).*

termination and orientation, which is not generally representative for the edge in the devices. The edge in our devices is randomly terminated with both zig-zag and armchair orientations. Furthermore, CVD-graphene sheets are usually multicrystalline, where various crystal orientations can be present in the active region of our devices. Using detailed electrochemical analyses, we have shown in our previous works that, in devices obtained using this fabrication strategy, the edge is exclusively in contact with the solution and the basal plane is well protected (see figure S3 in SI). [23-24] Figure 2b compares the typical field effect response in a buffer solution for a GrEdge-FET device (RPBW = 1 µm, red curve) with that of a cGFET device of comparable width (w = 1.2 µm, black curve). Although there are some subtle differences in the position of the Dirac point and the magnitude of the OFF resistance (defined as the resistance at the Dirac point, R_{Dirac}), it is clear that we obtain a similar field-effect as a cGFET just by gating only the edge. In order to ensure that we are really seeing the gating due to the edge (red curve in figure 2b), we have realized devices where both the basal plane and edge were covered with SU-8 completely. No field-effect or gate dependence of device resistance was measurable

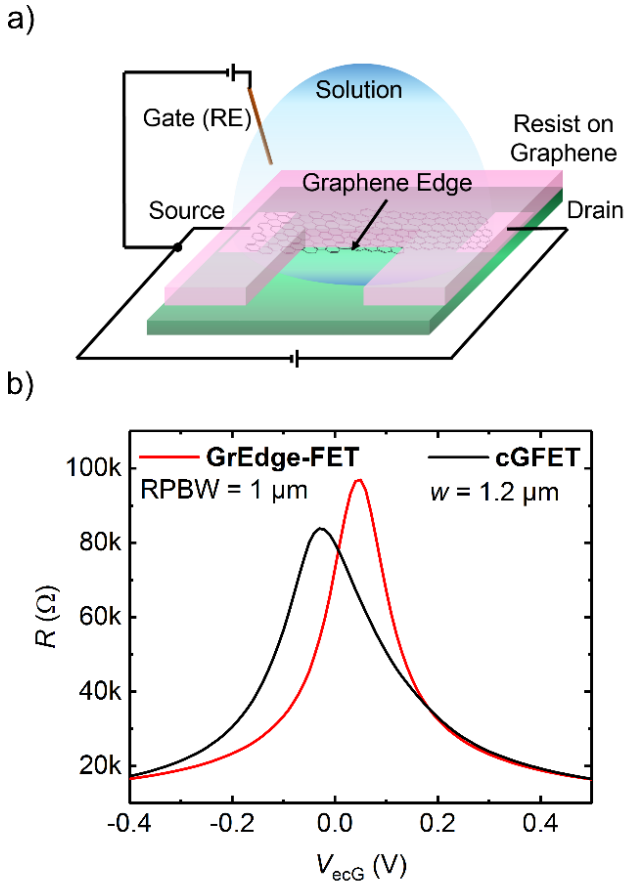

Figure 2: GrEdge-FET transfer characteristics. *a) A scheme of the gating setup, RE: reference electrode. b) Device resistance R as a function of gate voltage applied to the RE (electrochemical gate voltage, V_{ecG}) in solution for a GrEdge-FET with RPBW = 1 µm and a cGFET with w = 1.2 µm (phosphate buffer, pH 6.7, buffer concentration 10 mM, ionic strength 250 mM).*

in these devices (see figure S4 in SI for details). In comparison to cases where a very thin dielectric separates graphene from the electrolyte, [46] we have here a thick layer (~ 800 nm) of photoresist and hence do not expect gating to occur through the photoresist on the basal plane. In addition, AFM images (figure S2 in SI) clearly show that there is no basal plane exposed to the solution in the GrEdge-FETs. Based on these observations, it is quite clear that it is indeed possible to obtain a field-effect by gating the edge of the graphene sheet exclusively. Also in devices with larger RPBW, we could clearly see a gating exclusively through the edge (see figures S5 and S6 in SI). Previously, we have used surface-enhanced Raman spectroscopy (SERS) to decipher the chemical nature of the edge. Within the detection limit of SERS, we found little evidence for the presence of oxygen-rich functionalities. [24] On the other hand, the possibility of structural defects at the edge cannot be excluded.

From the measured curves, we have extracted ON/OFF values and estimated mobility using a modified Drude model (see figures S6 to S8 in SI and associated discussion). GrEdge-FETs with a given RPBW exhibit similar ON/OFF ratios and mobility as cGFETs of comparable channel width (w). We obtain a mean ON/OFF ratio of 7 for devices with RPBW = 1 μm and 8.5 for devices with RPBW = 0.75 μm, with one device reaching an ON/OFF ratio of 10. The lowest estimate of mobility is in the order of 300 cm^2/Vs, comparable to values reported for sub-30nm-wide GNRs. [12, 50] It is peculiar that we see such an effective gating in a low gate-voltage range, even though there is a considerable region of graphene support below the resist in parallel, which is not directly gated by the electrolyte. One possibility is that the electric field at the edge-electrolyte interface may gate not only the edge atoms, but also a region extending into the resist-protected graphene section. At a first sight, this picture is analogous to the observation of a depletion region induced by a side gate in graphene nanoribbon (GNR) FETs operating in air. [34, 37] In these devices, the gate-induced depletion region was found to be in the range of 90 nm for a field strength of 10^7 V/m. [34] Considering that the interfacial electric field in a GrEdge-FET is two orders of magnitude higher (> 0.5 V / nm), [39] it may be expected that the depletion width extending from the edge into the graphene sheet is considerably higher. However, at the edge-liquid interface, the electric field exists only at the EDL and we do not expect this field to affect the electrostatic potential profile far into the basal plane directly. [51] Also metal nanoparticle decoration has shown that the liquid exclusively accesses the edge (see figure S3 in SI). Hence, we believe that the gate-induced depletion region formed at the edge affects the charge distribution in the basal plane of the 2D sheet indirectly. This can be understood by considering that the charge carriers in the 2D graphene sheet are restricted to the single atomic layer and any disturbance of the Fermi level at the edge region will lead to a rapid equilibration of charges in the vicinity. This equilibration will eventually lead to a pinch-off of the channel similar to what is observed in classical MOSFETs. Our measurements indicate that the formation of the depletion region is effective for a width of several microns (as inferred

from GrEdge-FET devices with varying RPBW – see figure S5 and S6 in SI), most likely due to the 2D nature of electronic transport in our devices. Further support for this model is obtained from devices with passivated edges, where the basal plane was gated exclusively (see figure S9 for details). Also here a field-effect similar to that in a corresponding cGFET could be observed.

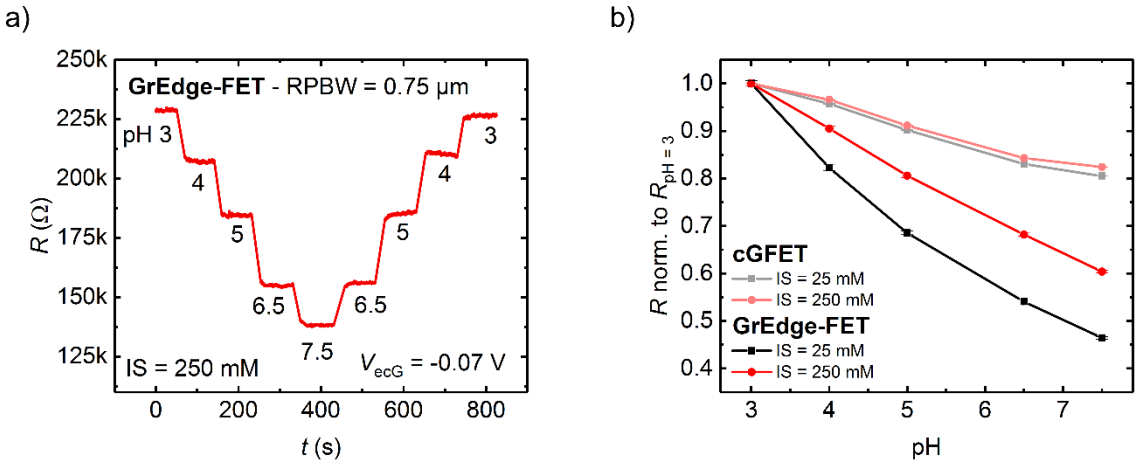

Figure 3: GrEdge-FET as pH sensor. *a) Device resistance R at a fixed gate voltage of V_{ecG} = -0.07 V for a GrEdge-FET device (with RPBW = 0.75 µm) as a function of pH of the buffer solution used (for all buffers: buffer concentration 10 mM, ionic strength IS = 250 mM). b) pH-dependent sensor response showing the relative change of R normalized to the value of R at pH 3 ($R_{pH = 3}$). The error bars depict the noise in the measurement in (a).*

Next, we evaluated the potential of using GrEdge-FETs as pH sensors. For this purpose, the resistance of the device in buffer solutions of varying pH were recorded at a constant gate voltage. The ionic strength was kept constant (either at 25 mM or at 250 mM) in all buffers in order to ensure that the thickness of the electrical double layer did not vary from one buffer to another. [40, 52] Figure 3a presents the pH response of the resistance for a typical GrEdge-FET with RPBW of 0.75 µm. A gate voltage lower than the Dirac point was chosen, where holes are the majority carriers. It is apparent that the resistance decreases as a function of solution pH. This is a result of the positive shift in Dirac point with increasing pH, which has been observed for cGFETs in several studies reported earlier. [9, 40-42, 46, 53-57] We have also estimated the isoelectric point (pI) of the edge-liquid interface using a methodology we have developed previously (see figure S10 and associated discussion in SI). [40] We observe that the GrEdge-electrolyte interface is negatively charged at all investigated pH values suggesting that the

isoelectric point or the point of zero charge is lower than 3, similar to what was observed on the basal plane. Figure 3b shows a typical comparison of the relative pH response obtained at a GrEdge-FET to that at a cGFET, for two different values of ionic strength, with the response being normalized to the resistance R at pH = 3. It is apparent that the sensitivity towards pH is higher for the GrEdge-FET than for a cGFET. It is worth mentioning that the GrEdge-FET devices with RPBW $\leq$ 1 μm were found to be much more robust than cGFET devices of comparable width, as exemplified by the several rounds of sensor trials that these devices could withstand without significant changes in the field-effect characteristics. The cGFET devices with small w in the range of 1 to 2 μm were more susceptible to damage as the resistance typically increased rapidly during the sensor trials, most likely due to the long FET channels (10 μm) deployed here. These observations are consistent with encapsulated GFETs being generally more stable. [46] Furthermore, GrEdge-FET devices showed superior symmetry of the gate dependent transfer curve and did not show double-peaks or shoulders. Such practical aspects underline the potential of GrEdge-FET devices towards routine sensor applications.

Finally, we demonstrate the capability of modulating the pH sensitivity of GrEdge-FETs through electrochemical modification using aryl diazonium precursors. This is a widely used strategy for covalent attachment of a range of functionalities on basal graphene. [58-61] A schematic of the electrochemical modification strategy is sketched in figure 4a. 4-aminophenyl diazonium precursors are generated in situ by the diazotization of phenylene diamine via sodium nitrite in an acidic aqueous solution, [62-63] in which the device is immersed. The GrEdge acts as the working electrode in an electrochemical cell. In order to achieve a covalent attachment of the aminophenyl moieties [60, 64-65] the potential at the GrEdge is cycled to a value, where the electrochemical reduction takes place, as shown in figure 4b. The electrochemical modification was carried out three times with the same parameters. In each step, the voltage

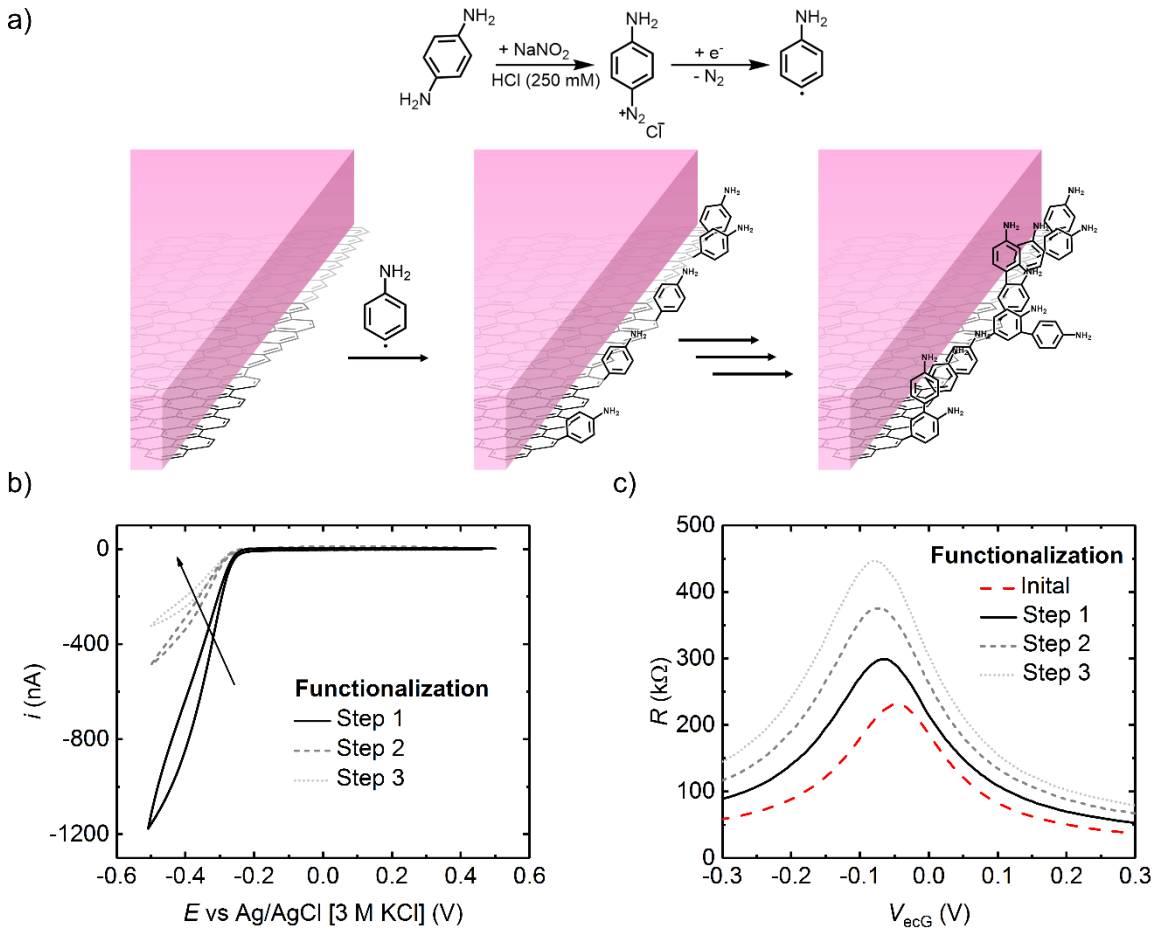

Figure 4: Covalent electrochemical modification of the graphene edge. *a) Scheme showing the covalent functionalization of the GrEdge with 4-aminophenyl residues. The diazonium species, generated via in-situ diazotization of p-phenylenediamine, is electrochemically reduced at the GrEdge used as the working electrode. The generation of aminophenyl radicals in local vicinity of the electrode results in covalent attachment at the GrEdge. b) Cyclic voltammetry (CV) was used to carry out the electrochemical reduction. The modification is performed three times. The first cycle of each functionalization step is shown. c) Gate-dependent transfer curves of a GrEdge-FET (RPBW = 0.75 µm) in the unmodified state (red, dashed line) and after each of the three functionalization steps (phosphate buffer pH 3, IS = 250 mM). The complete datasets for the modification in b) and the pH dependence in c) are shown in figure S11 in SI.*

was scanned for five cycles and the field-effect response measured subsequently (for detailed measurements, see figure S11 in SI). In the CVs in figure 4b, it is apparent that the cathodic current (for $E <$ -0.3V) decreases continuously with every modification step. This current contains contributions from the diazonium reduction. However, it is dominated by the current arising from the oxygen reduction reaction, which is typically observed for graphene electrodes in aqueous solution. [31, 66] The observed trend of reduction of the magnitude of cathodic current with every CV cycle suggests that the deposition of the diazonium-derived species at the edge gradually passivates the edge, hindering the possibility of electron transfer at the edge. [24, 26] We expect that the aminophenyl moieties attach selectively to the edge of the graphene sheet in a

covalent manner, since the rest of the graphene surface is passivated by the photoresist. [24] Evidence for this is obtained from Raman spectroscopy and FET data. That the basal plane in a GrEdge-FET does not undergo covalent modification is verified by Raman spectroscopy (see figures S12 and S13 in SI). Proof for covalent functionalization of the edge is further provided using cyclic voltammetry of a redox probe (see figure S14). The field-effect measurements (figure 4c) performed after every functionalization step are consistent with the obtained edge modification. Here, the resistance increases continuously with every modification. The ON/OFF ratio, however, remains around the value of 8 all along, while the apparent field-effect mobility decreases with every modification (see figure S15 in SI). Furthermore, the pI was found to be shifted to higher values after the modification (see figure S16). These data suggest that the active edge region is modified indeed covalently using the applied procedure.

Figure 5 presents a comparison of pH sensitivity at two different IS, showing the dependence of the Dirac point as a function of pH for the three different cases: cGFET, GrEdge-FET and functionalized GrEdge-FET. Although we cannot talk of a true linear response in the investigated pH range, [40] we can extract apparent slopes from the calibration curves, which are listed in Table 1. For cGFETs, the sensitivity is the lowest, with a low pH sensitivity of approx. 15 mV/pH at an ionic strength of 25mM, in line with previous reports. [41-42, 67-68] For GrEdge-

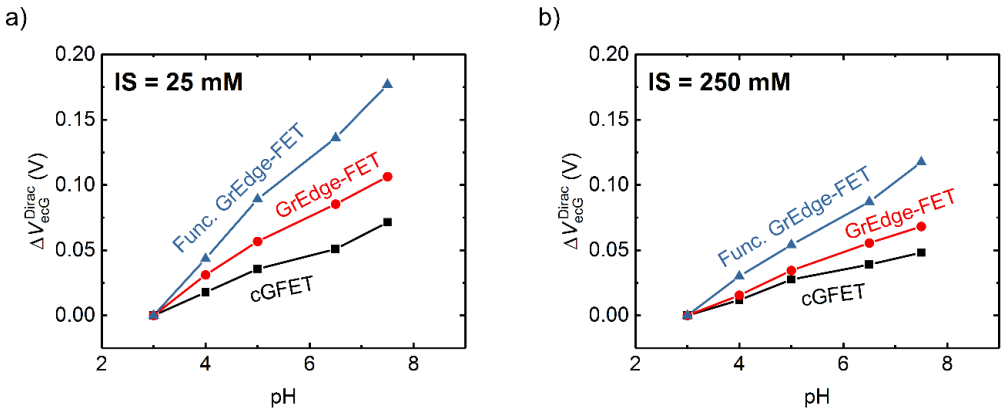

Figure 5: Comparison of pH sensitivity. *Relative shift of the Dirac point ΔV_{ecG}^{Dirac} as a function of pH in buffered solutions with fixed IS: a) 25mM b) 250 mM. The data measured with a conventional GFET (cGFET, w = 2.5 µm) are compared with a GrEdge-FET device (RPBW = 0.75 µm) in its initial state and after covalent modification (Func. GrEdge-FET) as outlined in figure 4. V_{ecG}^{Dirac} at pH 3 is used as the reference position of the Dirac point.*

FETs the pH sensitivity is around 23 mV/pH, while for the functionalized GrEdge-FETs we obtain a sensitivity as high as 39 mV/pH, the closest to the Nernstian limit of 59 mV/pH. This is around two times higher than previous reports on unmodified GFETs [41, 44, 68] and close to that obtained on Al_2O_3-encapsulated cGFETs. [46] For comparison, we have performed the covalent modification using the same 4-aminophenyl diazonium precursors on cGFET devices. Here, although the modification was successful as indicated by the Raman measurements (see figure S12 in SI), the pI of the basal graphene-liquid interface remained rather unaffected (see figure S17 in SI). Furthermore, the covalent modification results often in stark asymmetric transfer curves and non-reproducible transfer curve shifts and renders the extraction of Dirac point less reliable in cGFET devices (see figure S17 in SI). Finally, cGFET devices with channel width below 2 µm could not be functionalized covalently without destroying the channel. For the basal plane of graphene, a non-covalent attachment is more suited to obtain a sufficient density of surface functional groups, while retaining the favorable transfer characteristics of the GFET device. [40] On the contrary, in GrEdge-FETs with small RPBW, it is indeed possible with the help of covalent modification to obtain a high enough density to modify the chemistry of the interface. Most importantly, the favorable FET characteristics (ON resistance and ON/OFF ratio) could be preserved largely using such a covalent modification. It is worth mentioning that the functionalization had little effect on GrEdge-FETs with RPBWs higher than 10 µm (see figure S18 in SI). Moreover, the pH sensitivity was extremely poor in these devices.

Device	**Sensitivity (mV/pH)**	
	IS = 25 mM	*IS = 250 mM*
cGFET	15.2 ± 0.9	10.7 ± 0.8
GrEdge-FET	23.1 ± 1.3	15.3 ± 0.6
Func. GrEdge-FET	38.6 ± 1.5	25.3 ± 0.9

Table 1: *Apparent sensitivity of comparable GrEdge-FET (before and after covalent functionalization, RPBW = 0.75 µm) and cGFET (w = 2.5 µm) devices. The sensitivity is given as the slope of a linear fit through the data shown in figure 5, with the error being the uncertainty of the fit*

CONCLUSIONS

In summary, we have shown that a field-effect can be observed in a sheet of 2D-material when the one-dimensional edge is gated exclusively in a liquid environment. We achieved this gating by realizing a GrEdge-FET, wherein the basal plane is shielded by a thick photoresist and only the edge is exposed to the gating medium, which is an aqueous electrolyte. We observe that the electric field at the edge-electrolyte interface is efficient enough to modulate the charge carrier density in the entire graphene channel within a small gate voltage range of +/-0.5 V without any hysteresis in standard buffer solutions. While efficient gating appears to be possible for a graphene width up to several microns, the sensitivity of GrEdge-FETs is much higher for smaller channel width (RPBW), typically less than 1 micron and hence such narrow devices are more suitable for sensing applications. We showed that GrEdge-FETs can function as pH sensors, and that the pH sensitivity can be improved by covalent attachment of 4-aminophenyl residues. Although the apparent field-effect mobility is affected by the modification, other transfer characteristics such as the ON resistance and ON/OFF ratio could still be preserved. The sensitivity of such devices was shown to outperform conventional GFET devices with an open channel of comparable dimensions. Future work may focus on the selective detection of biomolecules at the GrEdge and the realization of GrEdge-FETs with a multitude of edges with the goal of improving the sensing performance.

EXPERIMENTAL SECTION

Device Fabrication. Devices were fabricated on silicon (100) wafers with 500 nm SiO_2 wet-oxide (*n*-type Si, dopant: antimony, 0.005-0.025 Ω cm, Siltron Inc. Korea). A maskless aligner HIMT MLA 100 (λ_{exc}: 365 nm) was used for photolithography. Positive photoresist S1805 (Microposit) was applied to the wafer by spin-coating and pre-baked for 2:20 min at 90°C. The layout was exposed (90 mJ/cm^2) and developed for 25 s in developer mf-319 (Microposit). Subsequently, 50 nm Ti and 10 nm Pt were evaporated onto the wafer. Thereafter, lift-off was

carried out in *N*-ethylpyrrolidone (NEP, ≥ 98 %, Roth) twice at 55°C, followed by acetone (VLSI, Selectipur®, BASF) and iso-propanol (≥ 99.9 %, VLSI, Roth), each with sonication for 30 minutes. Source and drain electrodes prepared in this manner had a separation with a 20 by 20 μm^2 gap, where the graphene channel was realized by transfer of CVD-grown monolayer graphene on Cu foil (Graphenea). Polystyrene (PS, av. Mw 35000, Aldrich) was applied on the graphene-on-copper foil by drop-casting from a solution in toluene (≥ 99.8 %, Rotisolv®, Roth) and dried for 15 min at 75°C. The etching of copper was carried out in a mixture of water (18.2 MΩ, Barnstead Easypure II), hydrochloric acid (37 w%, p.a., Emsure®, Merck) and hydrogen peroxide (30 %, p.a., AnalaR NORMAPUR, VWR) (16:3:1). After the transfer to the silicon chips, the samples were dried at 90°C for 20 min. PS was removed in toluene. The samples were then annealed at 600°C for 2 min in N_2 atmosphere. For patterning the transferred graphene, S1805 was used using the same procedure as above. Excess graphene was removed under oxygen plasma (0.5 mbar, 1 min). The passivation was realized using negative photoresist SU-8 (2) (MicroChem), which was spin coated (5000 rpm, 30 s) to obtain an approx. 800 nm film. The resist was then pre-baked at 65°C (2 min) and 95°C (5 min), exposed (300 mJ/cm^2), post-baked at 65°C (1 min) and 95°C (3 min), and developed in mrDev-600 (Micro Resist Technology) for 20 s. The samples were rinsed in iso-propanol and blow-dried in air. The open area of graphene in GrEdge-FETs was etched away under oxygen plasma (0.5 mbar, 18 s). The plasma had a light red color, which indicates that small amounts of nitrogen may also be present in the chamber.

Field-effect measurements. Field-effect measurements were performed using an Agilent E4980A Precision LCR-meter with an applied drain-source bias of 10 mV at a frequency of 1 kHz. An Ag/AgCl (3 M KCl) capillary reference electrode (WPI Dri-Ref-450) immersed in the buffer solution was used as the gate. The resistance (real part of the impedance) is recorded as a function of the applied gate voltage. The used buffer solutions were phosphate buffer (pH 3, 6.5, 6.7, 7.5) or acetate buffer (pH 4, 5), all of them with a buffer concentration (BC) of 10 mM. The total ionic strength (IS) of the buffer solutions was forced to either 25 mM or 250 mM using potassium chloride (≥ 99.0 %, Emprove® Essential, Merck). For the preparation of the buffer solution o-phosphoric acid (≥ 85 w%, p.a., Rotipuran®, Roth), potassium phosphate monobasic (≥ 99.0 %, Sigma), potassium phosphate dibasic (≥ 98.0 %, Sigma-Aldrich), acetic acid glacial (analytical reagent grade, Fisher Scientific) and sodium acetate anhydrous (≥ 98.5%, Serva) were used. Prior to the first measurement on each device, e-etching in 100 mM HCl was performed to remove trace Cu residues. [66, 69]

In situ diazotization and electrochemical modification. For covalent modification, 4-aminophenyl diazonium cations were generated *in-situ* and electrochemically reduced to 4-aminophenyl radicals. A solution of 2 mM *p*-phenylenediamine (98 %, Sigma-Aldrich) in 0.5 M HCl and a solution of 3 mM sodium nitrite (≥ 98 %, Alfa Aesar) were prepared and mixed 1:1 directly at 4°C prior to the electrochemical modification. [62-63] Upon mixing, the solution turned yellow indicating the formation of 4-aminophenyl diazonium chloride. The electrochemical modification was performed in a standard three-electrode set-up using an Ivium Compactstat potentiostat. A Pt wire was used as the counter electrode, an Ag/AgCl (3 M KCl) capillary reference electrode served as the reference electrode.

Graphene Characterization. Raman measurements were performed using a JASCO NRS-4100 Raman spectrometer (1650·256 CCD detector (Andor; air/Peltier-cooled to -60°C); grating with 900 Lines/mm; green laser with λ = 532 nm at 5.6 mW power; 100x (NA 0.90) objective). A NanoScope Dimension 3100 in tapping mode or JPK Nanowizard 4 was used for AFM imaging.

SUPPORTING INFORMATION

Optical images of fabrication steps; AFM images of GrEdge-FET device; control experiment on cGFET device with fully covered channel; control experiment on cGFET device with passivated edges; comparison of evolution of resistance parameters of cGFET and GrEdge-FET as a function of RPBW; modified Drude model; Raman analysis of unmodified and modified cGFET device; Raman analysis of modified GrEdge-FET; complete dataset of modification and pH-tests on GrEdge-FET device with small RPBW; evolution of model parameters after the functionalization steps of GrEdge-FET; pH tests and covalent modification of cGFET devices with different widths; pH sensitivity of GrEdge-FET device with high RPBW.

COMPETING INTERESTS

The authors declare no competing interests.

ACKNOWLEDGEMENTS

Funding from the German Science Foundation (DFG) via the Graduate School of Analytical Sciences Adlershof (SALSA GSC1013) and via grant INST 276/754-1 is acknowledged. We acknowledge Stephan Schmid and Birgit Lemke of MPI Stuttgart, Martin Muske of HZB and Michael Winterfeld of HU Berlin for help with metal deposition, wafer dicing and lithography.

REFERENCES

1. Geim, A. K.; Novoselov, K. S., The rise of graphene. *Nat. Mater.* **2007,** *6* (3), 183-191.
2. Romagnoli, M.; Sorianello, V.; Midrio, M.; Koppens, F. H. L.; Huyghebaert, C.; Neumaier, D.; Galli, P.; Templ, W.; D'Errico, A.; Ferrari, A. C., Graphene-based integrated photonics for next-generation datacom and telecom. *Nat. Rev. Mater.* **2018,** *3* (10), 392-414.
3. Ferrari, A. C.; Bonaccorso, F.; Fal'ko, V.; Novoselov, K. S.; Roche, S.; Bøggild, P.; Borini, S.; Koppens, F. H. L.; Palermo, V.; Pugno, N.; Garrido, J. A.; Sordan, R.; Bianco, A.; Ballerini, L.; Prato, M.; Lidorikis, E.; Kivioja, J.; Marinelli, C.; Ryhänen, T.; Morpurgo, A.; Coleman, J. N.; Nicolosi, V.; Colombo, L.; Fert, A.; Garcia-Hernandez, M.; Bachtold, A.; Schneider, G. F.; Guinea, F.; Dekker, C.; Barbone, M.; Sun, Z.; Galiotis, C.; Grigorenko, A. N.; Konstantatos, G.; Kis, A.; Katsnelson, M.; Vandersypen, L.; Loiseau, A.; Morandi, V.; Neumaier, D.; Treossi, E.; Pellegrini, V.; Polini, M.; Tredicucci, A.; Williams, G. M.; Hee Hong, B.; Ahn, J.-H.; Min Kim, J.; Zirath, H.; van Wees, B. J.; van der Zant, H.; Occhipinti, L.; Di Matteo, A.; Kinloch, I. A.; Seyller, T.; Quesnel, E.; Feng, X.; Teo, K.; Rupesinghe, N.; Hakonen, P.; Neil, S. R. T.; Tannock, Q.; Löfwander, T.; Kinaret, J., Science and technology roadmap for graphene, related two-dimensional crystals, and hybrid systems. *Nanoscale* **2015,** *7* (11), 4598-4810.
4. Li, J.; Niu, L.; Zheng, Z.; Yan, F., Photosensitive Graphene Transistors. *Adv. Mater.* **2014,** *26* (31), 5239-5273.
5. Balasubramanian, K.; Kern, K., 25th Anniversary Article: Label-Free Electrical Biodetection Using Carbon Nanostructures. *Adv. Mater.* **2014,** *26* (8), 1154-1175.
6. Neumaier, D.; Zirath, H., High frequency graphene transistors: can a beauty become a cash cow? *2D Mater.* **2015,** *2* (3), 030203.
7. Béraud, A.; Sauvage, M.; Bazán, C. M.; Tie, M.; Bencherif, A.; Bouilly, D., Graphene field-effect transistors as bioanalytical sensors: design, operation and performance. *Analyst* **2021,** *146* (2), 403-428.
8. Jia, X.; Campos-Delgado, J.; Terrones, M.; Meunier, V.; Dresselhaus, M. S., Graphene edges: a review of their fabrication and characterization. *Nanoscale* **2011,** *3* (1), 86-95.
9. Tan, X.; Chuang, H.-J.; Lin, M.-W.; Zhou, Z.; Cheng, M. M.-C., Edge Effects on the pH Response of Graphene Nanoribbon Field Effect Transistors. *J. Phys. Chem. C* **2013,** *117* (51), 27155-27160.
10. Chen, Z.; Lin, Y.-M.; Rooks, M. J.; Avouris, P., Graphene nano-ribbon electronics. *Physica E: Low-dimensional Systems and Nanostructures* **2007,** *40* (2), 228-232.
11. Xie, G.; Shi, Z.; Yang, R.; Liu, D.; Yang, W.; Cheng, M.; Wang, D.; Shi, D.; Zhang, G., Graphene Edge Lithography. *Nano Lett.* **2012,** *12* (9), 4642-4646.
12. Wang, X.; Ouyang, Y.; Li, X.; Wang, H.; Guo, J.; Dai, H., Room-temperature all-semiconducting sub-10-nm graphene nanoribbon field-effect transistors. *Phys. Rev. Lett.* **2008,** *100* (20), 206803.
13. Li, X.; Wang, X.; Zhang, L.; Lee, S.; Dai, H., Chemically Derived, Ultrasmooth Graphene Nanoribbon Semiconductors. *Science* **2008,** *319* (5867), 1229.
14. Kwon, S. S.; Shin, J. H.; Choi, J.; Nam, S.; Park, W. I., Defect-Mediated Molecular Interaction and Charge Transfer in Graphene Mesh-Glucose Sensors. *ACS Appl. Mater. Interf.* **2017,** *9* (16), 14216-14221.
15. Sandner, A.; Preis, T.; Schell, C.; Giudici, P.; Watanabe, K.; Taniguchi, T.; Weiss, D.; Eroms, J., Ballistic Transport in Graphene Antidot Lattices. *Nano Lett.* **2015,** *15* (12), 8402-8406.
16. Traversi, F.; Raillon, C.; Benameur, S. M.; Liu, K.; Khlybov, S.; Tosun, M.; Krasnozhon, D.; Kis, A.; Radenovic, A., Detecting the translocation of DNA through a nanopore using graphene nanoribbons. *Nat. Nanotechnol.* **2013,** *8*, 939.

17. Ritter, K. A.; Lyding, J. W., The influence of edge structure on the electronic properties of graphene quantum dots and nanoribbons. *Nat. Mater.* **2009,** *8* (3), 235-242.
18. Xu, W.; Lee, T.-W., Recent progress in fabrication techniques of graphene nanoribbons. *Mater. Horiz.* **2016,** *3* (3), 186-207.
19. Jessen, B. S.; Gammelgaard, L.; Thomsen, M. R.; Mackenzie, D. M. A.; Thomsen, J. D.; Caridad, J. M.; Duegaard, E.; Watanabe, K.; Taniguchi, T.; Booth, T. J.; Pedersen, T. G.; Jauho, A.-P.; Bøggild, P., Lithographic band structure engineering of graphene. *Nat. Nanotechnol.* **2019,** *14* (4), 340-346.
20. Acik, M.; Chabal, Y. J., Nature of Graphene Edges: A Review. *Jpn. J. Appl. Phys.* **2011,** *50* (7), 070101.
21. Zhang, X.; Xin, J.; Ding, F., The edges of graphene. *Nanoscale* **2013,** *5* (7), 2556-2569.
22. Fujii, S.; Enoki, T., Nanographene and Graphene Edges: Electronic Structure and Nanofabrication. *Acc. Chem. Res.* **2013,** *46*, 2202.
23. Yadav, A.; Wehrhold, M.; Neubert, T. J.; Iost, R. M.; Balasubramanian, K., Fast Electron Transfer Kinetics at an Isolated Graphene Edge Nanoelectrode with and without Nanoparticles: Implications for Sensing Electroactive Species. *ACS Appl. Nano Mater.* **2020,** *3* (12), 11725-11735.
24. Yadav, A.; Iost, Rodrigo M.; Neubert, T. J.; Baylan, S.; Schmid, T.; Balasubramanian, K., Selective electrochemical functionalization of the graphene edge. *Chem. Sci.* **2019,** *10* (3), 936-942.
25. Caridad, J. M.; Calogero, G.; Pedrinazzi, P.; Santos, J. E.; Impellizzeri, A.; Gunst, T.; Booth, T. J.; Sordan, R.; Bøggild, P.; Brandbyge, M., A Graphene-Edge Ferroelectric Molecular Switch. *Nano Lett.* **2018,** *18* (8), 4675-4683.
26. Bellunato, A.; Schneider, G. F., Electrophilic Radical Coupling at the Edge of Graphene. *Nanoscale* **2018,** *10*, 12011.
27. Jiang, J.; Zhang, P.; Liu, Y.; Luo, H., A novel non-enzymatic glucose sensor based on a Cu-nanoparticle-modified graphene edge nanoelectrode. *Anal. Methods* **2017,** *9*, 2205.
28. Tao, L.; Wang, Q.; Dou, S.; Ma, Z.; Huo, J.; Wang, S.; Dai, L., Edge-rich and Dopant-free Graphene as a Highly Efficient Metal-Free Electrocatalyst for the Oxygen Reduction Reaction. *Chem. Commun.* **2016,** *52*, 2764.
29. Li, K.; Jiang, J.; Dong, Z.; Luo, H.; Qu, L., A Linear Graphene Edge Nanoelectrode. *Chem. Commun.* **2015,** *51*, 8765.
30. Banerjee, S.; Shim, J.; Rivera, J.; Jin, X.; Estrada, D.; Solovyeva, V.; You, X.; Pak, J.; Pop, E.; Aluru, N.; Bashir, R., Electrochemistry at the Edge of a Single Graphene Layer in a Nanopore. *ACS Nano* **2013,** *7*, 834.
31. Shen, A.; Zou, Y.; Wang, Q.; Dryfe, R. A. W.; Huang, X.; Dou, S.; Dai, L.; Wang, S., Oxygen Reduction Reaction in a Droplet on Graphite: Direct Evidence that the Edge Is More Active than the Basal Plane. *Angew. Chem., Int. Ed.* **2014,** *53*, 10804.
32. Yuan, W.; Zhou, Y.; Li, Y.; Li, C.; Peng, H.; Zhang, J.; Liu, Z.; Dai, L.; Shi, G., The Edge- and Basal-plane-Specific Electrochemistry of a Single-Layer Graphene Sheet. *Sci. Rep.* **2013,** *3*, 2248.
33. Macedo, L. J. A.; Iost, R. M.; Hassan, A.; Balasubramanian, K.; Crespilho, F. N., Bioelectronics and Interfaces Using Monolayer Graphene. *ChemElectroChem* **2019,** *6* (1), 31-59.
34. Molitor, F.; Güttinger, J.; Stampfer, C.; Graf, D.; Ihn, T.; Ensslin, K., Local gating of a graphene Hall bar by graphene side gates. *Phys. Rev. B* **2007,** *76* (24), 245426.
35. Chen, C.; Low, T.; Chiu, H.; Zhu, W., Graphene-Side-Gate Engineering. *IEEE Electron Dev. Lett.* **2012,** *33* (3), 330-332.
36. Hähnlein, B.; Händel, B.; Schwierz, F.; Pezoldt, J., Properties of Graphene Side Gate Transistors. *Mater. Sci. Forum* **2013,** *740-742*, 1028-1031.

37. Panchal, V.; Lartsev, A.; Manzin, A.; Yakimova, R.; Tzalenchuk, A.; Kazakova, O., Visualisation of edge effects in side-gated graphene nanodevices. *Sci. Rep.* **2014,** *4* (1), 5881.
38. Hwang, W. S.; Zhao, P.; Kim, S. G.; Yan, R.; Klimeck, G.; Seabaugh, A.; Fullerton-Shirey, S. K.; Xing, H. G.; Jena, D., Room-Temperature Graphene-Nanoribbon Tunneling Field-Effect Transistors. *npj 2D Mater. Appl.* **2019,** *3* (1), 43.
39. Xu, K.; Fullerton-Shirey, S. K., Electric-double-layer-gated transistors based on two-dimensional crystals: recent approaches and advances. *J. Phys. Mater.* **2020,** *3* (3), 032001.
40. Zuccaro, L.; Krieg, J.; Desideri, A.; Kern, K.; Balasubramanian, K., Tuning the isoelectric point of graphene by electrochemical functionalization. *Sci. Rep.* **2015,** *5*, srep11794.
41. Fu, W.; Nef, C.; Knopfmacher, O.; Tarasov, A.; Weiss, M.; Calame, M.; Schönenberger, C., Graphene Transistors Are Insensitive to pH Changes in Solution. *Nano Lett.* **2011,** *11* (9), 3597-3600.
42. Ohno, Y.; Maehashi, K.; Yamashiro, Y.; Matsumoto, K., Electrolyte-gated graphene field-effect transistors for detecting pH and protein adsorption. *Nano Lett.* **2009,** *9* (9), 3318-3322.
43. Mailly-Giacchetti, B.; Hsu, A.; Wang, H.; Vinciguerra, V.; Pappalardo, F.; Occhipinti, L.; Guidetti, E.; Coffa, S.; Kong, J.; Palacios, T., pH sensing properties of graphene solution-gated field-effect transistors. *J. Appl. Phys.* **2013,** *114* (8), 084505.
44. Kaiser, D.; Tang, Z.; Küllmer, M.; Neumann, C.; Winter, A.; Kahle, R.; Georgi, L.; Weimann, T.; Siegmann, M.; Gräfe, S.; Centeno, A.; Zurutuza, A.; Turchanin, A., pH sensors based on amino-terminated carbon nanomembrane and single-layer graphene van der Waals heterostructures. *Applied Physics Reviews* **2021,** *8* (3), 031410.
45. Ang, P. K.; Chen, W.; Wee, A. T. S.; Loh, K. P., Solution-Gated Epitaxial Graphene as pH Sensor. *J. Am. Chem. Soc.* **2008,** *130* (44), 14392-14393.
46. Fakih, I.; Mahvash, F.; Siaj, M.; Szkopek, T., Sensitive Precise p H Measurement with Large-Area Graphene Field-Effect Transistors at the Quantum-Capacitance Limit. *Phys. Rev. Appl.* **2017,** *8* (4), 044022.
47. Georgakilas, V.; Otyepka, M.; Bourlinos, A. B.; Chandra, V.; Kim, N.; Kemp, K. C.; Hobza, P.; Zboril, R.; Kim, K. S., Functionalization of Graphene: Covalent and Non-Covalent Approaches, Derivatives and Applications. *Chem. Rev.* **2012,** *112* (11), 6156-6214.
48. Bekyarova, E.; Sarkar, S.; Wang, F.; Itkis, M. E.; Kalinina, I.; Tian, X.; Haddon, R. C., Effect of Covalent Chemistry on the Electronic Structure and Properties of Carbon Nanotubes and Graphene. *Acc. Chem. Res.* **2013,** *46* (1), 65-76.
49. Zhang, H.; Bekyarova, E.; Huang, J.-W.; Zhao, Z.; Bao, W.; Wang, F.; Haddon, R. C.; Lau, C. N., Aryl Functionalization as a Route to Band Gap Engineering in Single Layer Graphene Devices. *Nano Lett.* **2011,** *11* (10), 4047-4051.
50. Yang, Y.; Murali, R., Impact of Size Effect on Graphene Nanoribbon Transport. *IEEE Electron Dev. Lett.* **2010,** *31* (3), 237-239.
51. Allen J. Bard, L. R. F., *Electrochemical Methods: Fundamentals and Applications*. 2nd ed. ed.; Wiley: 2000.
52. Heller, I.; Chatoor, S.; Männik, J.; Zevenbergen, M. A. G.; Dekker, C.; Lemay, S. G., Influence of Electrolyte Composition on Liquid-Gated Carbon Nanotube and Graphene Transistors. *J. Am. Chem. Soc.* **2010,** *132* (48), 17149-17156.
53. Han, D.; Chand, R.; Kim, Y. S., Microscale loop-mediated isothermal amplification of viral DNA with real-time monitoring on solution-gated graphene FET microchip. *Biosens. Bioelectron.* **2017,** *93*, 220-225.
54. Mitsuno, T.; Taniguchi, Y.; Ohno, Y.; Nagase, M., Ion sensitivity of large-area epitaxial graphene film on SiC substrate. *Appl. Phys. Lett.* **2017,** *111* (21), 213103.
55. Kwon, S. S.; Shin, J. H.; Choi, J.; Nam, S.; Park, W. I., Nanotube-on-graphene heterostructures for three-dimensional nano/bio-interface. *Sens. Actuat. B* **2018,** *254*, 16-20.

56. Piccinini, E.; Bliem, C.; Reiner-Rozman, C.; Battaglini, F.; Azzaroni, O.; Knoll, W., Enzyme-polyelectrolyte multilayer assemblies on reduced graphene oxide field-effect transistors for biosensing applications. *Biosens. Bioelectron.* **2017,** *92*, 661-667.
57. Fenoy, G. E.; Marmisollé, W. A.; Azzaroni, O.; Knoll, W., Acetylcholine biosensor based on the electrochemical functionalization of graphene field-effect transistors. *Biosens. Bioelectron.* **2020,** *148*.
58. Rösicke, F.; Gluba, M. A.; Shaykhutdinov, T.; Sun, G.; Kratz, C.; Rappich, J.; Hinrichs, K.; Nickel, N. H., Functionalization of any substrate using covalently modified large area CVD graphene. *Chem. Commun.* **2017,** *53* (67), 9308-9311.
59. Greenwood, J.; Phan, T. H.; Fujita, Y.; Li, Z.; Ivasenko, O.; Vanderlinden, W.; Van Gorp, H.; Frederickx, W.; Lu, G.; Tahara, K.; Tobe, Y.; Uji-i, H.; Mertens, S. F. L.; De Feyter, S., Covalent Modification of Graphene and Graphite Using Diazonium Chemistry: Tunable Grafting and Nanomanipulation. *ACS Nano* **2015,** *9* (5), 5520-5535.
60. Paulus, G. L. C.; Wang, Q. H.; Strano, M. S., Covalent Electron Transfer Chemistry of Graphene with Diazonium Salts. *Acc. Chem. Res.* **2013,** *46* (1), 160-170.
61. Niyogi, S.; Bekyarova, E.; Hong, J.; Khizroev, S.; Berger, C.; de Heer, W.; Haddon, R. C., Covalent Chemistry for Graphene Electronics. *J. Phys. Chem. Lett.* **2011,** *2* (19), 2487-2498.
62. Lyskawa, J.; Bélanger, D., Direct Modification of a Gold Electrode with Aminophenyl Groups by Electrochemical Reduction of in Situ Generated Aminophenyl Monodiazonium Cations. *Chem. Mater.* **2006,** *18* (20), 4755-4763.
63. Rösicke, F.; Sun, G.; Neubert, T.; Janietz, S.; Hinrichs, K.; Rappich, J., Electrochemical functionalization of Au by aminobenzene and 2-aminotoluene. *J. Phys.: Cond. Mat.* **2016,** *28* (9), 094004.
64. Lim, H.; Lee, J. S.; Shin, H.-J.; Shin, H. S.; Choi, H. C., Spatially Resolved Spontaneous Reactivity of Diazonium Salt on Edge and Basal Plane of Graphene without Surfactant and Its Doping Effect. *Langmuir* **2010,** *26* (14), 12278-12284.
65. Bellunato, A.; Arjmandi Tash, H.; Cesa, Y.; Schneider, G. F., Chemistry at the Edge of Graphene. *ChemPhysChem* **2016,** *17* (6), 785-801.
66. Iost, R. M.; Crespilho, F. N.; Zuccaro, L.; Yu, H. K.; Wodtke, A. M.; Kern, K.; Balasubramanian, K., Enhancing the Electrochemical and Electronic Performance of CVD-Grown Graphene by Minimizing Trace Metal Impurities. *ChemElectroChem* **2014,** *1* (12), 2070-2074.
67. Cheng, Z.; Li, Q.; Li, Z.; Zhou, Q.; Fang, Y., Suspended Graphene Sensors with Improved Signal and Reduced Noise. *Nano Lett.* **2010,** *10* (5), 1864-1868.
68. Ristein, J.; Zhang, W.; Speck, F.; Ostler, M.; Ley, L.; Seyller, T., Characteristics of solution gated field effect transistors on the basis of epitaxial graphene on silicon carbide. *J. Phys. D: Appl. Phys.* **2010,** *43* (34), 345303.
69. Neubert, T. J.; Wehrhold, M.; Kaya, N. S.; Balasubramanian, K., Faradaic effects in electrochemically gated graphene sensors in the presence of redox active molecules. *Nanotechnol.* **2020,** *31* (40), 405201.